

Effect of the Surface modification of Cellulose nanofibers on the Mechanical Properties and Disintegrability of Specific PLA/Cellulose Composites

Justyna Wietecha¹, Janusz Kazimierczak¹, Agata Jeziorna^{1*}

¹ Łukasiewicz – Lodz Institute of Technology, 19/27 M. Skłodowska-Curie Str., 90-570 Łódź, Poland

* Corresponding author. E-mail: agata.jeziorna@it.lukasiewicz.gov.pl

Abstract

PLA/nanofibrillar cellulose (NFC) composite films were produced by solution casting. Before use, the cellulose fibers were modified with various types of surface active agents – cationic, anionic and non-ionic surfactants. The structure and morphology of samples of the cellulose fillers and composite films with polymer were analyzed by means of scanning electron microscopy and PXRD diffraction. Thermal parameters of the composite films were characterized by differential scanning calorimetry and thermogravimetric analysis. The tensile strength and elongation at break of the films were evaluated in mechanical tests. The ability to disintegrate of all PLA/NFC composites under composting conditions was also determined and compared.

Keywords

PLA, cellulose nanofibres, surfactants, green composites.

1. Introduction

In the modern sustainable economy, an important need is the use of polymers based on natural resources in place of traditional plastics from the processing of fossil raw materials, since the post-use waste of the latter is often difficult to manage and creates a burden for the environment. Growing public awareness of the environmental threats and more and more restrictive legal regulations stimulate interest in biodegradable polymers, which, unlike most traditional synthetic polymers produced from crude oil, decompose in the natural environment [1]. The biodegradability of synthetic and natural polymers is determined by their chemical structure, while the rate of biodegradation of objects made of them, apart from parameters such as temperature and humidity, is also influenced by their shape and specific surface area. The biodegradation of polymers is significantly favoured by low crystallinity, low molecular weight, the presence of chemical groups susceptible to the action of appropriate enzymes and/or environmental factors, as well as the absorption of water by the polymer as a means of enzyme and/or ion transport. Functional groups that are subject to enzymatic hydrolysis and oxidation are present in the chains of biodegradable polymers, such as aliphatic polyesters,

including polylactide (PLA) (Figure 1) [2].

PLA is synthesized by ring-opening polymerization of a cyclic dimer or by direct condensation polymerization of lactic acid monomers [3, 4]. Lactic acid, the substrate for PLA production, can be obtained on an industrial scale, in an ecological approach, by fermentation of mono- or di-saccharides derived from renewable resources, such as sugar cane or corn starch with the participation of lactic acid bacteria. The energy required to produce a unit of mass is about 50% lower in the case of PLA compared to petroleum-based plastics such as polypropylene (PP), low-density polyethylene (LDPE), polystyrene (PS) and polyamide (PA) [5].

PLA is completely biodegradable under industrial composting conditions and its degradation products are metabolized by microorganisms [6]. It is estimated

that the complete biodegradation of PLA takes from six months to two years, while the biodegradation time of synthetic polymers such as PE or PS is between 500 and 1000 years [7]. Due to its biocompatibility and non-toxic features, PLA could be used, among others, in food packaging, drug delivery systems and scaffolds for tissue engineering [8–10]. PLA polymers can also be processed into a wide range of fibrous materials used in the production of woven and knitted fabrics [11]. PLA has a high tensile strength and Young modulus, but it suffers from such drawbacks as inherent brittleness, low toughness, low heat resistance, poor processability, barrier properties and foamability, which result from its slow crystallization rate and low melt strength [3, 12–15].

The properties of PLA need to be improved in order to increase the range of its applications in the fields where traditional polymers are still used. One

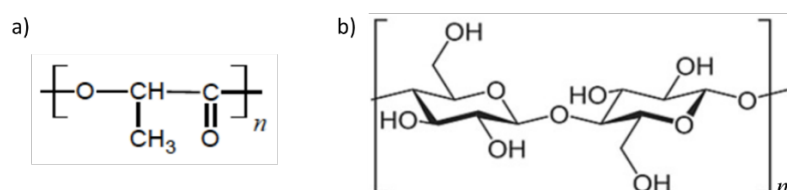


Fig. 1. Chemical structure of a) polylactide chain, b) cellulose chain

of the ways to improve the mechanical and chemical properties of biodegradable polymers can include the incorporation of nanostructured fillers, which can act as mechanical reinforcement of the polymer structure. Natural cellulose nanofibers may be an option for this functionalization because of their low density, high toughness, low cost and biodegradability [8, 16]. Nanocellulose can be divided into three main categories: nanocrystalline cellulose (NCC), nanofibrillated cellulose (NFC), and bacterial nanocellulose (BNC) [17]. While both NCC and NFC are produced through top-down methods using chemical, physical, and enzymatic processes, BNC production relies on the bottom-up process of cellulose synthesis by bacterial strains, such as *Komagataeibacter xylinus*, in a glucose-rich culture medium. NFC manufacturing also implements the concept of sustainable economy as it can be produced by isolation and extraction from the by-products of agriculture and forestry [18].

Bio-composites of PLA reinforced with NFC have been extensively investigated, and studies revealed that due to the polarity difference of PLA and NFC, good dispersibility of NFC in the PLA matrix is often challenging. The studies mainly focused on decreasing the NFC surface hydrophilicity and polarity and hence improving its dispersion within hydrophobic polymeric matrices. Generally, three strategies of surface modification are performed on NFC to reinforce PLA-based composites: physical adsorption of a surfactant, chemical derivatization, and chemical grafting of PLA [19-24].

Polymer-cellulose nanocomposites can be produced by various processes, which can also affect the properties of the target composite and determine the purpose of its use [25].

In the scientific literature, most of the research conducted for this type of composite concerns the Ingeo PLA 2000 [26, 27] and PLA 4000 series [28], which are specifically designed for use in fresh food packaging.

In our study, we used Ingeo™ 6201D PLA polymer (NatureWorks® LLC) to produce a series of PLA/nanocellulose composite films. PLA Ingeo™ 6201D (NatureWorks® LLC) is a thermoplastic fibrous resin that is well suited for fibre production where lower fiber shrinkage is desired. Potential applications of the Ingeo biopolymer 6000 series are the production of fiberfills, nonwovens, agricultural woven and nonwoven fabrics, as well as disposable household articles. Moreover, this grade of Ingeo biopolymer has also been approved by the U.S. Food and Drug Administration (FDA) for use in food packaging materials. Products made of it can be used for all types of food and use conditions [29].

This research was focused on improving the physical adsorption and affinity between PLA Ingeo™ 6201D and NFC by adding surface active agents. Due to the dual nature of surfactants, they are commonly used in interfacial processes, such as foaming, wetting and emulsifying, as well as in detergents. In solid composites, they can also act as an interfacial compatibilizer. In a PLA/NFC composite, the hydrophilic end of the surfactant can bind to the NFC nanofibrils, while the hydrophobic side will interact with the polymer component. The authors decided to use commercial and certified chemicals that would support homogenization of the core components. Surfactants of various nature were selected, such as the mixture of partially saponified fatty acid methyl esters of castor oil (ZS1) as an anionic surfactant, the very popular cationic surfactant cetyltrimethylammonium bromide (CTAB), and sucrose palmitate RYOTO™ P 1670 as a non-ionic emulsifier with HLB (hydrophilic-lipophilic balance) of *ca.* 16. Easy access to all components of guaranteed quality is important to the overall production and industrial applications of the composites designed.

Despite the great interest of scientists and research progress in the field of green composite design, there are still significant difficulties in the large-scale production of such composite materials. In addition, the results of other researchers published regarding

the use of cellulose as a reinforcement of PLA matrix are sometimes inconsistent, which may indicate many important, though subtle, variables, not only in the selection of ingredients [30]. It is well known that the physical and mechanical properties of materials are closely related to the manufacturing and post-processing conditions [31]. Therefore, additional research is still needed in this area.

The authors' efforts were concerned with investigating how surface modifications of cellulose nanofibers with different surfactants actually affect the properties of PLA Ingeo™ 6201D/cellulose composite film.

2. Experimental section

2.1. Materials

Chloroform of analytical grade was purchased from POCh, Poland as a solvent for the preparation of PLA solution and NFC suspensions.

Poly(lactic acid) (PLA) in the form of pellets was supplied by NatureWorks® LLC as PLA Ingeo™ 6201D polymer. Selected physicochemical properties of PLA 6201D according to the manufacturer's data are summarized in Table 1 [32]. The chemical purity of this material was verified in a study by Józwicka et al. [33].

Cellulose nanofibres (NFC) were prepared at Łukasiewicz – Lodz Institute of Technology, Łódź, Poland. NFC was extracted from pulp derived from hemp stalks. The crude pulp was pretreated using cellulolytic enzymes (endoglucanases) to weaken interactions between individual microfibrils. Enzymatic treatment promotes the mechanical breakdown of pulp fibers, reducing the amount of energy needed for this process. Next,

Density, g/cm ³	1,24
Melting point, °C	155-170
Glass transition point, °C	55-60
Contents of D-lactide isomer(%)	1,4

Table 1. Physicochemical characteristics of PLA 6201D

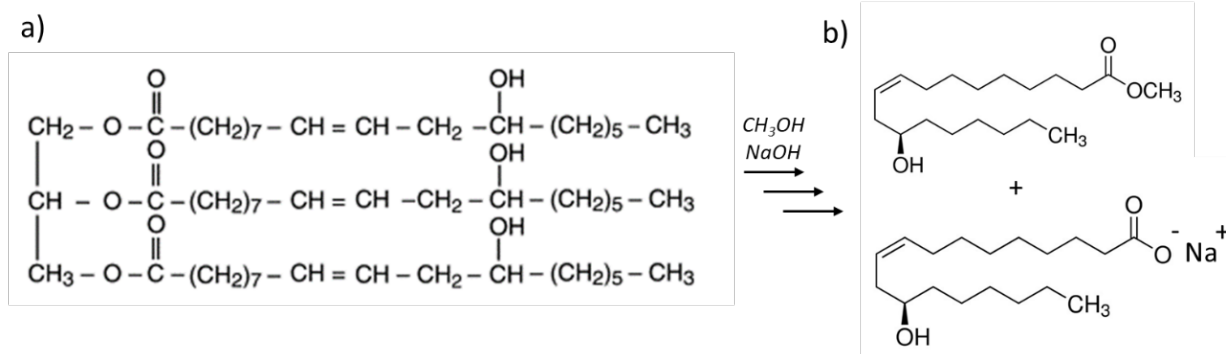


Fig. 2. Partially saponified fatty acid methyl esters of castor oil – ZS1 (simplified formula). a) Structure of ricinoleic acid as the main component of castor oil; b) possible products of the transesterification reaction of ricinoleic acid

the aqueous suspension of the pulp was subjected to high mechanical shearing in a CAT, X1740 homogenizing system using a DK40 flow-through chamber equipped with a cooling system. In the last step, the NFC was isolated from the slurry by centrifugation (Hettich, Rotina 420) at 4500 rpm and partially concentrated on a rotary evaporator (Büchi, Rotavapor R-300).

Partially saponified fatty acid methyl esters of castor oil (ZS1) were supplied by the Łukasiewicz-Institute of Heavy Organic Synthesis, Kędzierzyn-Koźle, Poland. Castor oil is a mixture of (tri-, di-, mono-) glycerides of fatty acids, i.e. ricinoleic acid (90%), oleic acid, linoleic acid and others. Methyl esters are usually obtained in the process of transesterification of oils with methyl alcohol in the presence of an alkaline catalyst. ZS1 belongs to the group of anionic surfactants (Figure 2).

Cetyltrimethylammonium bromide (CTAB) was purchased from J&K Scientific, USA. CTAB, a cationic surfactant, like others, forms micelles in aqueous solutions (Figure 3)

Sucrose palmitate RYOTO™ P-1670 was supplied by Mitsubishi Chemical Foods Co. Sucrose esters are non-ionic carbohydrate surfactants obtained by the esterification of sucrose with fatty acids. The sucrose moiety is polar and acts as the hydrophilic end of the molecule, while the long fatty acid chain is its lipophilic end. Due to this amphipathic property, sucrose esters act as universal emulsifiers (Figure 4).

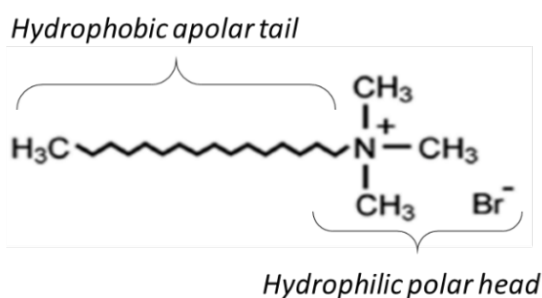


Fig. 3. Chemical structure of CTAB

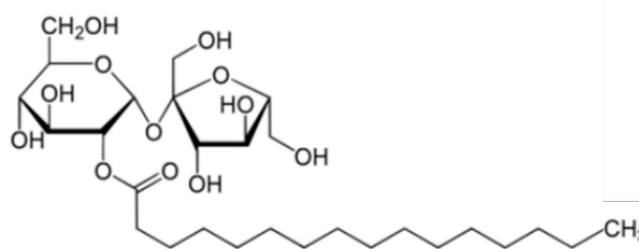


Fig. 4. Chemical structure of sucrose palmitate - P1670

Compost "Próchniaczek" used for the disintegrability test was supplied by the Waste Management Board in Lodz, Poland. It is obtained from the selective organic fraction of municipal waste as a result of the aerobic decomposition of biomass by the action of microorganisms.

2.2. Methods

The morphology of the modified cellulose particles was characterized using a FESEM scanning electron microscope (FEI, Quanta 200) at an electron beam accelerating voltage of 10 kV. Prior to SEM analysis, the samples were gold

sputtered using a Q150R vacuum coater from Quorum Technologies.

The structural changes of NFC/surfactants and characteristics of the inert structure of polymeric composite foils were specified by X-ray diffraction (XRD) analysis. PXRD experiments were registered on a Panalytical Empyrean powder X-Ray diffractometer using copper radiation ($\lambda = 1.5419 \text{ \AA}$) and zero-background holders. The 2θ range in each case was $5\text{--}45^\circ$.

The UV-vis transmittance of the PLANFC composite films prepared was examined from 200 to 800 nm by a Thermo Spectronic, Helios γ spectrophotometer.

TGA and DSC analyses were performed to evaluate the thermal properties of PLA composite films using a Setaram, TG Labsys Evo 1150 instrument with “Calisto” AKTS control and processing software. Analysis parameters: atmosphere - oxygen-free nitrogen, flow 20 cm³/min; vessel - Pt 100 μl; heating rate - 10 K/min; temperature range - 20 - 200°C

Tensile tests of pure PLA and PLA NFC composite films were carried out under standard environmental conditions (temperature 20±2°C and relative humidity 65±4 %). The following parameters were estimated: tensile strength and elongation at break. The measurements were made using an Instron 5544 tensile tester. Three specimens were tested per each sample. Specimen measuring section length: 50 mm, stretching speed: 100 mm/min, sample width: 15 mm.

A disintegration test was carried out following the PN-EN ISO 20200:2007 standard by the accredited Laboratory of Biodegradation and Microbiological Research at Łukasiewicz – Łódź Institute of Technology, Poland.

2.3. Preparation of NFC and surface modified NFC

NFC was mixed with three different compatibilizers at a ratio of 9:1 (w/w) based on dry weight. The functionalized cellulose materials (NFC/ZS1; NFC/CTAB; NFC/P1670) were then spray-dried (GEA, MOBILE MINOR®) to give powder forms that could be used in combination with hydrophobic polymer matrices.

2.4. Preparation of PLA/NFC composite films

In screw-capped bottles, appropriate amounts of each of the functionalized cellulose samples i.e. NFC/ZS1, NFC/CTAB, and NFC/P1670 was dispersed in chloroform using a handheld homogenizer (CAT, X 120). A 10 % solution of PLA in chloroform was prepared in another

vessel. All samples were then sonicated to eliminate NFC or PLA aggregates and possibly air bubbles. In the next step, a proportional amount of PLA solution was added to each NFC suspension sample, then mixed on a shaker and again subjected to ultrasound. The final concentration of PLA in chloroform was 5 % and the concentration of modified NFC - 10 % in relation to the dry weight of PLA. The resulting compositions (45 g) were poured into shallow rectangular molds (16×16 cm) and air-dried in a fume hood for *ca.* 3-5 days. The formed PLA/NFC films were then placed in a desiccator under a vacuum for 48 hours to completely remove the organic solvent from the composite mass.

In the same way, reference samples were prepared in the form of PLA with NCF filling without a carrier of surfactants, marked as PLA NFC/0, and film made of pure PLA. The initially transparent layer of pure PLA became opaque during storage in a desiccator. For comparative tests, we also used a transparent PLA film, i.e. dried only in air at atmospheric pressure. The reference samples of pure PLA were named PLA *crystalline* and PLA *amorphous*, respectively, which corresponded to their crystalline structure, confirmed by PXRD analysis during further studies.

2.5. Disintegration test under composting conditions

Decomposition studies of pure PLA films and PLA composites with cellulose modified with different types of surfactants obtained by casting the solution were conducted under simulated composting conditions with controlled temperature and humidity. The samples were weighed and transferred to reaction nets, which were placed in a research reactor filled with compost for a period of 14 days. After the allotted time, the samples were weighed and put back to continue the experiment for one week. The compost used in the biodegradation tests was characterized by moisture in the range of 40-65 % and biological activity (total number of microorganisms) not lower than 10E6 cfu/g. The reactor was

placed in a climate chamber. Moisture loss was monitored and replenished daily.

3. Results and discussion

3.1. Morphology and structure characterization of modified NFC fibers.

A microscopic analysis of the morphology of NFC surfaces modified with various surfactants is shown in Figure 5. After spray drying, all NFC samples in the form of powder had a shape similar to a spherical one with a folded surface. According to the scale bar in the SEM images, the particle diameters were in the range of 0.85-10.6 μm; but the particle size of the fraction modified with the anionic surfactant ZS1 seemed slightly larger compared to the NFC particles modified with other reagents, i.e. cationic CTAB and non-ionic P1670.

PXRD diffraction was used to analyze changes in the crystal structure of cellulose fibers under the influence of the surfactants. In Figure 6, a set of PXRD patterns for unmodified and surfactant-modified NFC fibers can be seen with virtually no difference in the peak shape or intensity for individual samples. Observable peaks at $2\theta = 15^\circ, 17^\circ, 22^\circ$ and 34° correspond to (101), (101 $\bar{1}$), (002) and (040) planes, respectively, and are typical of the cellulose I structure [34]. The PXRD result clearly indicates that surfactant molecules penetrating the cellulose fibers do not affect the crystalline domains of the cellulose structure.

In order to check whether NFC functionalizing substances have a protective effect on cellulose during NFC drying, preventing so-called keratosis, samples of the surfactant modified NFC powders were re-dispersed in water and air-dried. Keratosis is a physical process involving structural changes occurring as a result of the progress of degradation of the amorphous phase in cellulose fibers, e.g. as a result of spray drying. This may result in the shortening and weakening of mechanical properties of cellulose fibres. Figures 7 a-c show SEM images

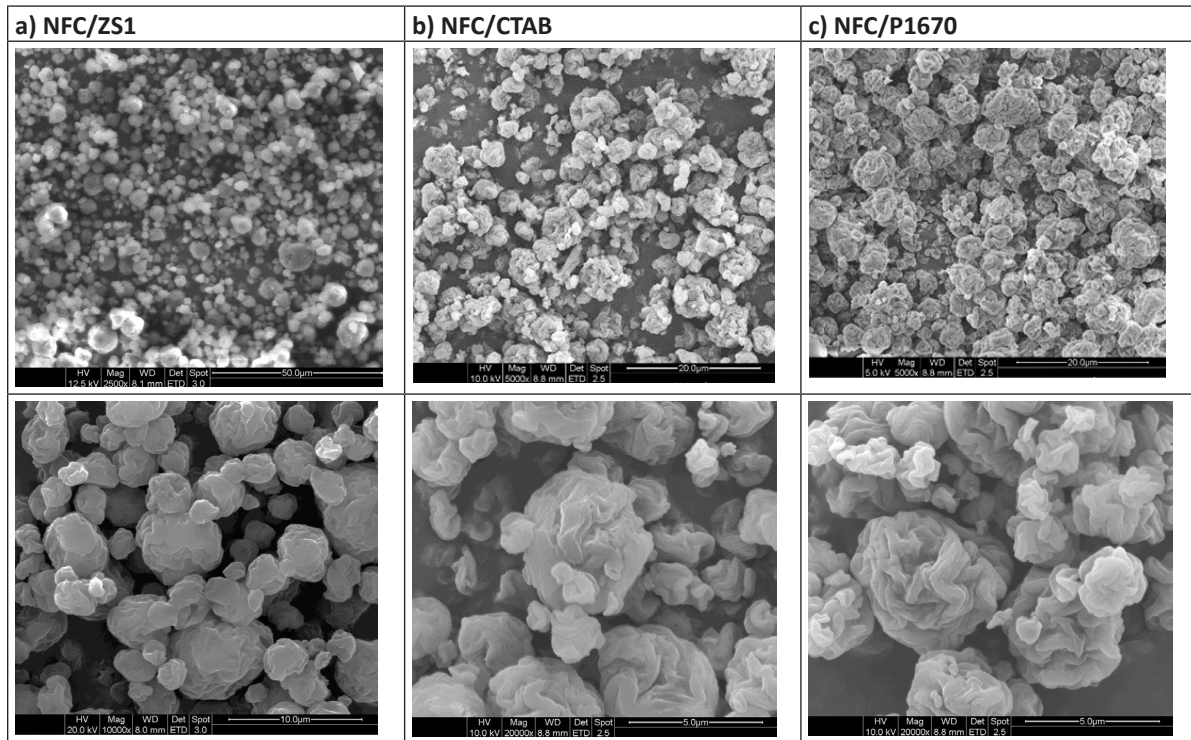


Fig. 5. SEM images of NFC samples functionalized with three different compatibilizers after spray drying; a) NFC/ZS1 – 50 μm scale bar (upper picture) and 10 μm (lower picture); b) NFC/CTAB – 20 μm scale bar (upper picture) and 5 μm (lower picture); c) NFC/P1670 – 20 μm scale bar (upper picture) and 5 μm (lower picture)

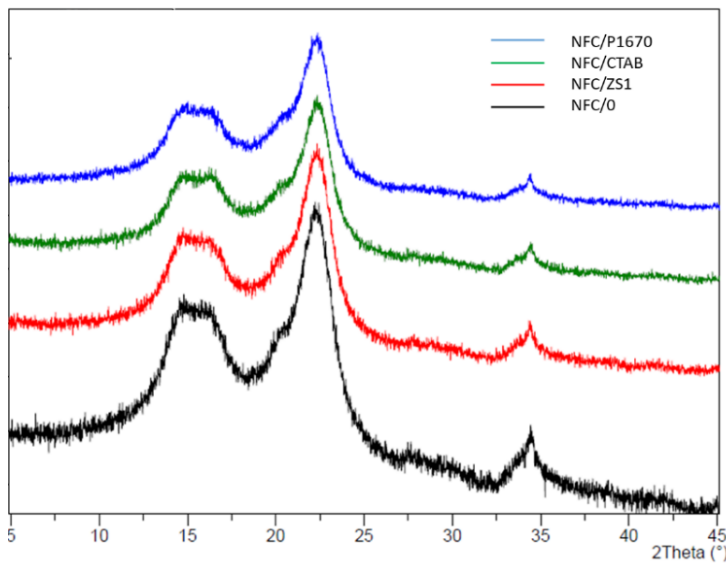


Fig. 6. Comparison of PXRD diffractograms of unmodified and surfactant modified NFC powder samples

of re-dispersed surfactant modified NFC particles.

As can be seen from the SEM images, NFC/ZS1 and NFC/CTAB particles regained their fibrous structure after re-dispersing in water, although in the case of NFC/P1670 the structure recovery was the least visible.

3.2. Morphology and structure characterization of PLA NFC composite films

Samples of 14x14 cm were cut out of the formed films in order to eliminate possible inhomogeneities and deformations of the foil related to the edge effect on the walls of the forming vessel. The

thickness of each PLA film was about 0.1 mm. Pictures of the composite films and reference samples of pure PLA in an amorphous and crystalline form are shown in Figure 8.

Macroscopic optical evaluation of the composite film obtained showed transparency only for the pure PLA film formed at ambient temperature and pressure. The addition of CNF significantly reduced the light permeability of the composite membranes, which was consistent with the optical observations in both visible and UV wavelengths (see Figure 9). The pure PLA film held under a vacuum to completely remove the organic solvent from the polymer pulp; like the PLA NFC composites samples, it was also less transparent.

PLA/NFC composite and pure PLA films were also characterized by PXRD analysis. The diffractograms presented in Figure 10 indicate the crystalline structure of pure PLA film probably obtained by diffusion of chloroform from a transparent amorphous PLA film.

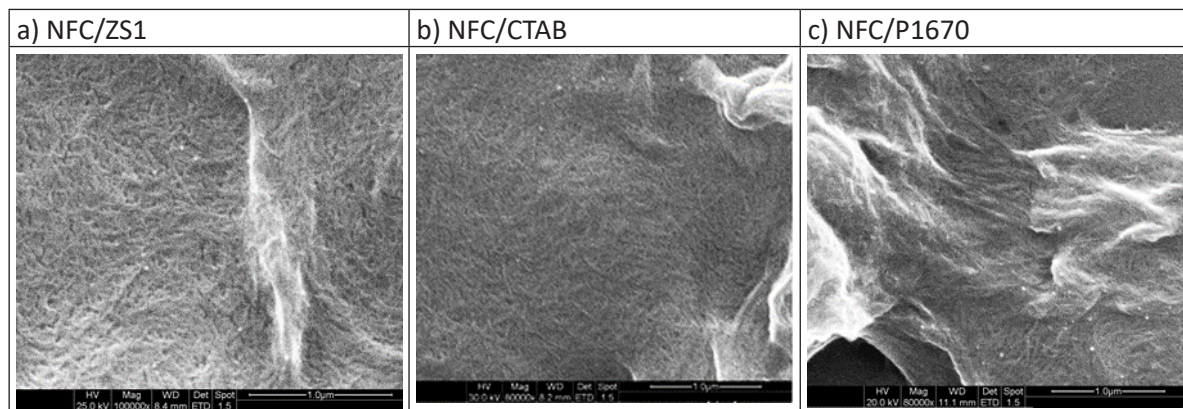


Fig. 7. SEM images of particles of cellulose nanofibers modified with surfactants after re-dispersion in water: a) NFC/ZS1, b) NFC/CTAB, c) NFC/P1670

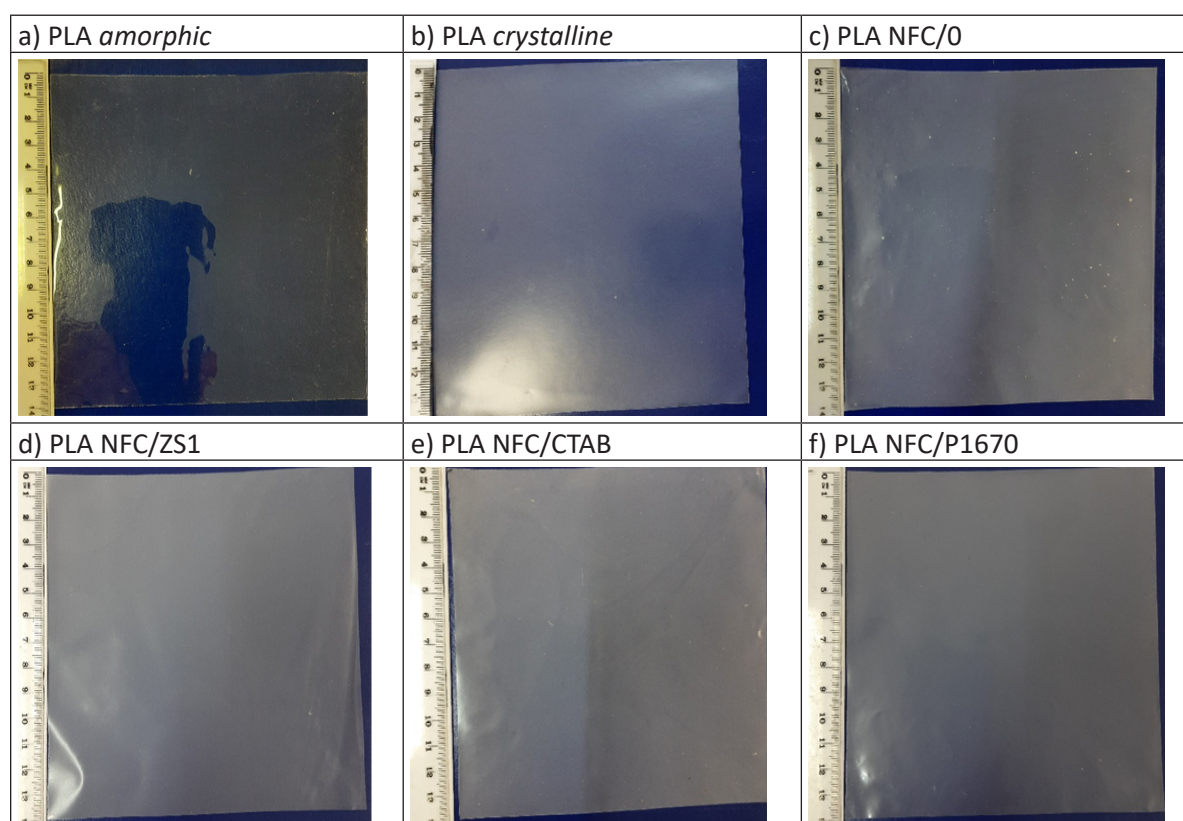


Fig. 8. Photos of composite foils (c-f) and reference samples of pure PLA (a-b)

Pure PLA crystal as a reference sample was obtained under the conditions in which the composite films with cellulose additives were prepared. In the last stage, all foil samples were placed in a chamber with reduced pressure to get rid of chloroform residues. Solvent vapors escaping from the polymer matrix could favor the ordering of polymer chains through the nucleation and growth of crystals in the matrix. Interestingly, such a phenomenon occurred only for the foil not filled with cellulose particles. NFC-

containing samples remained practically amorphous or at most semi-crystalline. In the diffraction pattern of the transparent PLA amorphous film, only a characteristic broad peak at 16° is observed, which may indicate semi-crystallization during processing. The difference between the diffraction patterns of both reference samples made of pure PLA is evident and can be helpful in the analysis of the PLA/NFC composite structure after forming the foil.

The addition of NFC fibers, both in the unchanged form and after modification with surfactants, causes slight changes in the diffraction pattern, i.e. the appearance of convexities on the spectral line at the angles $2\theta=17^\circ$ and 23° in relation to the spectrum of the amorphous form of PLA. The highest proliferation of the peak at $2\theta=23^\circ$ can be observed in the diffraction pattern of the PLA NFC/ZS1 sample. It is known from the literature that the addition of nanocellulose to the polymer matrix may increase PLA crystallinity as

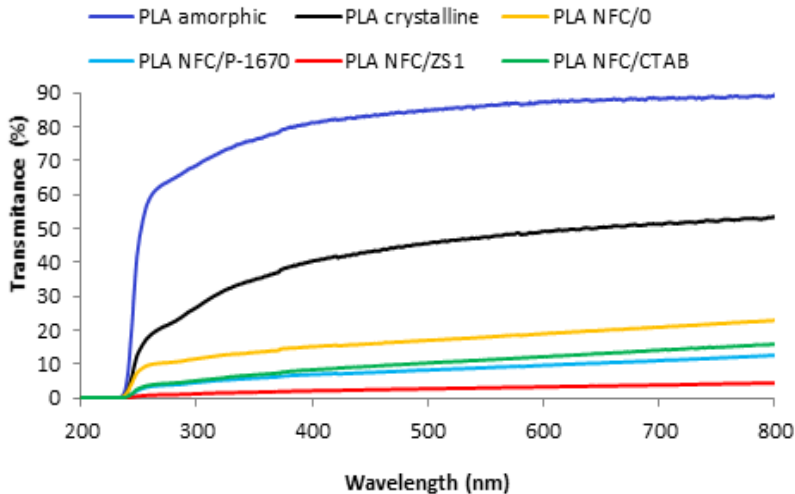


Fig. 9. Optical transmittance of neat PLA and PLA CNF composite films (with CNF fibers modified with various surfactants)

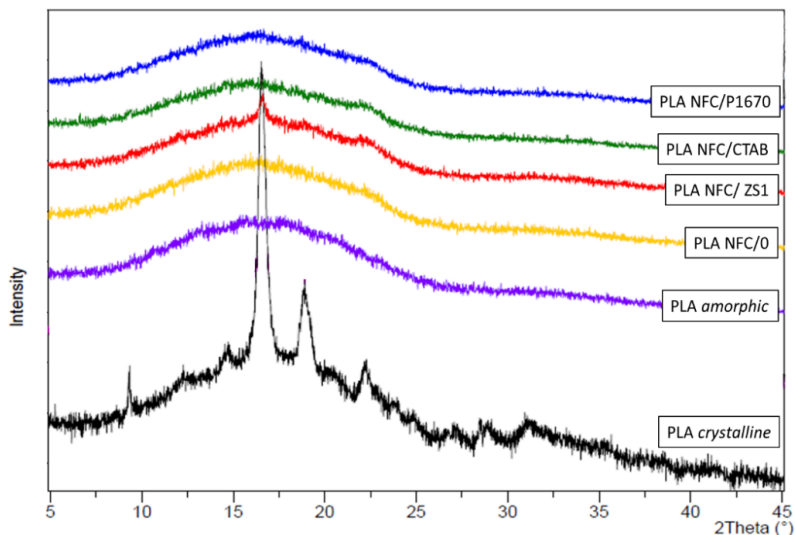


Fig. 10. PXRD diffractograms of pure PLA and PLA NFC/surfactants films

a result of the introduction of additional crystallization nuclei [26]. However, the changes observed in the spectrum may come from diffraction peaks of NFC crystals, largely masked by the wide diffraction peak of PLA.

3.3. Evaluation of thermal properties of PLA NFC films

Thermal properties of neat PLA and PLA NFC composite films were characterized by DSC and TG techniques. The full DSC curves of the first heating in the range of 20-200 °C and the corresponding TGA plots for all samples are shown in Figure 11.

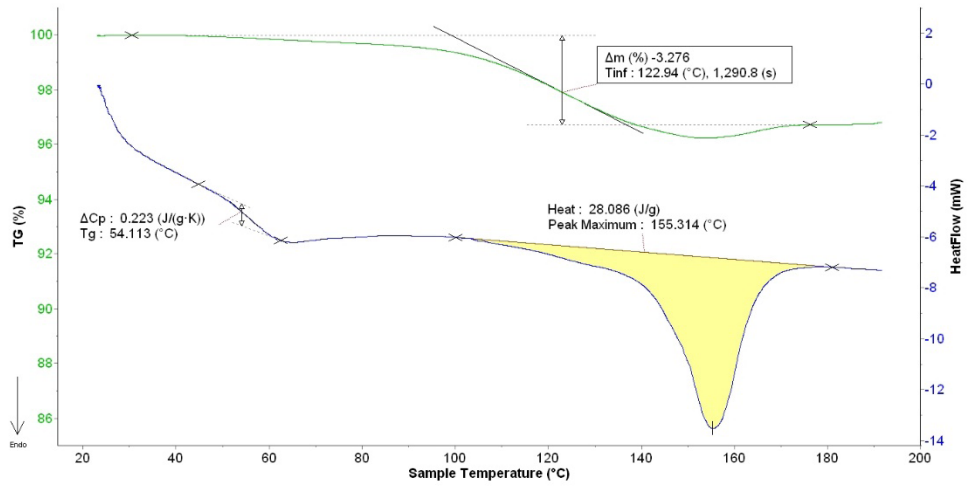
The thermal parameters from the DSC analysis, such as the glass transition temperature (T_g), cold crystallization temperature (T_{cc}), melting temperature (T_m) and appropriate enthalpies ΔH_{cc} (cold crystallization enthalpy) and ΔH_m (melting enthalpy) are summarized in Table 2. TGA data are also shown in Table 2, indicating differences in temperature ranges ($T_1 - T_{inf} - T_2$) and weight loss (Δm) between PLA and PLA NFC composites during the release of residual chloroform. Checchetto et al. confirmed that the desorption process of residual solvent from PLA films occurs in the temperature range from T_g to T_m (DSC), where TG evidences the first mass loss [35].

The DSC profile of the PLA *crystalline* sample is characterized by a strong endothermic peak associated with melting at $T_m = 155^\circ\text{C}$, which indicates a highly crystalline structure, and the glass transition peak (C_p) is the smallest and at a slightly lower temperature (T_g) compared to other PLA films tested. According to the TG at 20-200°C, this sample is characterized by the lowest weight loss ($\Delta m = -3.3\%$), which proves the highest degree of solvent removal from the sample mass during film formation (conditioning in a vacuum desiccator).

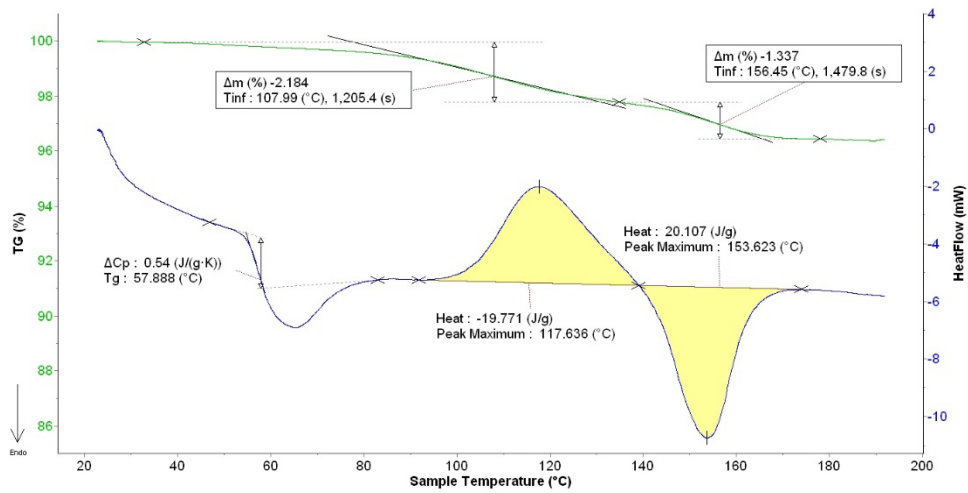
The DSC pattern of the amorphous pure PLA film (PLA *amorphous*) confirmed its character, although the enthalpies of melting and cold crystallization are not completely balanced ($\Delta H_{cc} + \Delta H_m = 0.3\text{ J/g}$), which would indicate a low content of crystal structure. Traces of crystallinity in the sample are also recognized by a weaker glass transition stroke (change in heat capacity, $\Delta C_p = 0.54\text{ J/g}\cdot\text{K}$) compared to other amorphous samples. The PLA *amorphous* film is the only one of the samples tested to show two stages of weight loss during heating at 20-200°C (see TG plot), but the total weight loss ($\Delta m = -3.5\%$) is not greater than for the others, although the cast PLA *amorphous* film was not placed in a vacuum chamber during post-processing. This result is probably due to two different types of interactions between chloroform molecules and PLA chains in the polymer matrix.

The amorphous structures of all composite films containing the NFC additive (PLA NFC/0, PLA NFC/ZS1, PLA NFC/CTAB, PLA NFC/P1670) were confirmed by the following features of DSC profiles: strong glass transitions, where the specific heat values (C_p) are *ca.* $0.6\text{ J/g}\cdot\text{K}$, as well as the balancing effects of cold crystallization and melting ($\Delta H_{cc} + \Delta H_m = 0.0\text{ J/g}$). The addition of unmodified NFC particles to the PLA matrix (see TG for PLA NFC/0 sample) shifts the desolvation temperature towards lower values as compared to the PLA crystalline sample prepared under the same conditions (vacuum post-processing). On the other hand, the release of residual solvent from PLA

a) PLA crystalline



b) PLA amorphous



c) PLA NFC/0

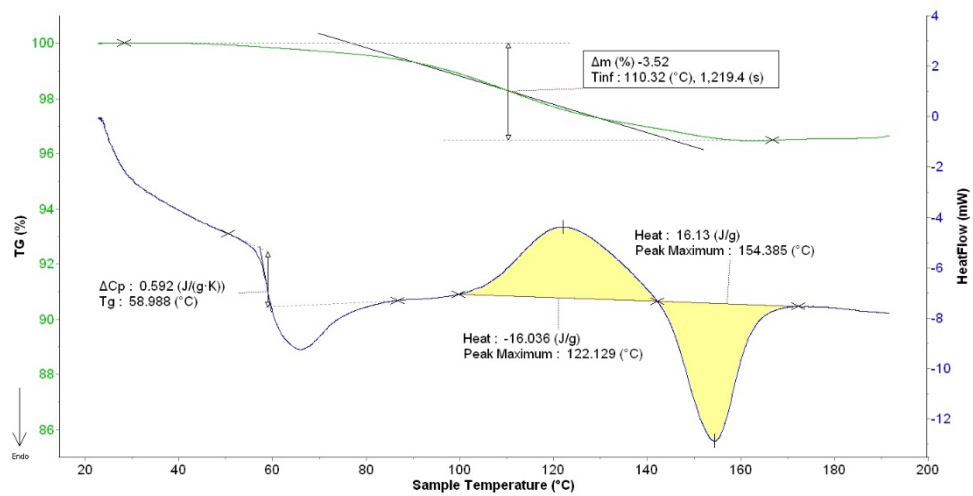
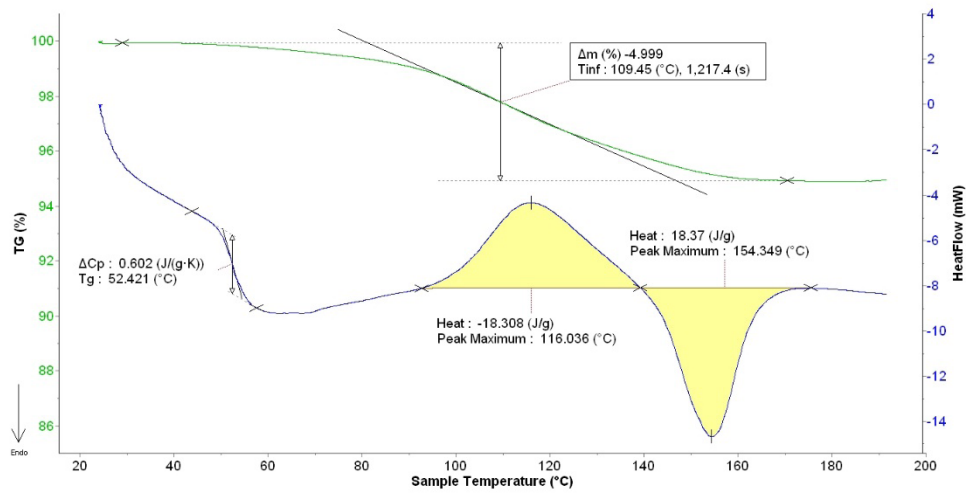
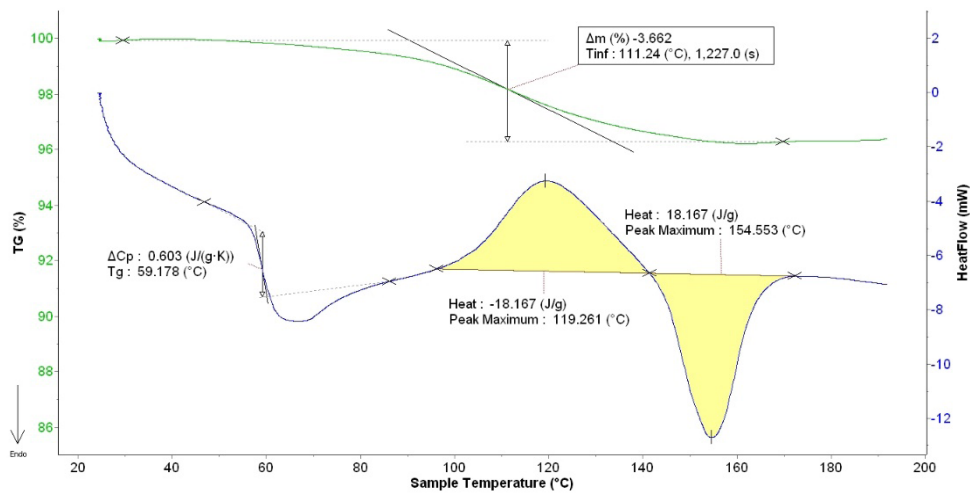


Fig. 11. DSC (bottom blue line) and TG (top green line) graphs of pure PLA (a-b) and PLA with unmodified NFC (c) and PLA NFC/surfactants films (d-f)

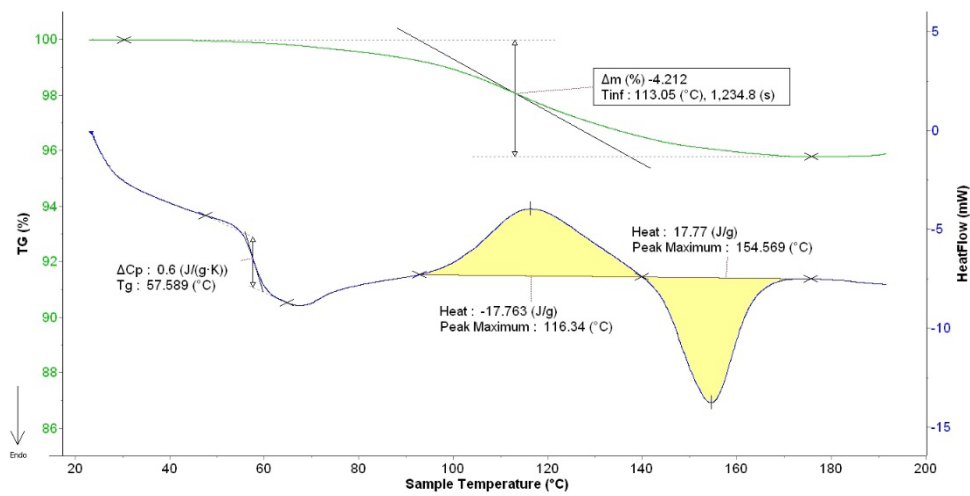
d) PLA NFC/ZS1



e) PLA NFC/CTAB



f) PLA NFC/P1670



Continued Fig. 11. DSC (bottom blue line) and TG (top green line) graphs of pure PLA (a-b) and PLA with unmodified NFC (c) and PLA NFC/surfactants films (d-f)

Sample	TG				DSC						
	T ₁ [°C]	T _{inf} [°C]	T ₂ [°C]	Δm [%]	T _g [°C]	ΔC _p [J/g*K]	T _{cc} [°C]	ΔH _{cc} [J/g]	T _m [°C]	ΔH _m [J/g]	
PLA _{crystalline}	99,1	122,9	136,7	-3,3	54,1	0,22	-	-	155,3	28,1	
PLA _{amorphous}	77,6	108,0	130,9	-2,2	57,9	0,54	117,6	-19,8	153,6	20,1	
	142,5	156,5	165,5	-1,3							
PLA NFC/0	76,6	110,3	145,3	-3,5	59,0	0,59	122,1	-16,0	154,4	16,1	
PLA NFC/ZS1	81,5	109,5	147,0	-5,0	52,4	0,60	116,0	-18,3	154,3	18,4	
PLA NFC/CTAB	90,3	111,2	133,8	-3,7	59,2	0,60	119,3	-18,2	154,6	18,2	
PLA NFC/P 1670	92,6	113,1	137,4	-4,2	57,6	0,60	116,3	-17,8	154,6	17,8	

Table 2. TGA and DSC thermal characteristic of pure PLA and PLA NFC/surfactant composites

film with NFC filling modified with surfactants (PLA NFC/ZS1, PLA NFC/CTAB, PLA NFC/P1670) starts at higher temperatures and results in greater weight loss of samples during heating at 20-200°C.

According to TG, the PLA NFC/ZS1 composite foil shows the highest weight loss compared to the other foils tested ($\Delta m = 5\%$). This sample is characterized by the lowest glass transition temperature, which, combined with the largest weight loss, would indicate a higher content and weaker binding of the substance volatiles in the PLA matrix. Probably, the slightly larger particles of NFC/ZS1 compared to NFC/CTAB and NFC/1670 (see Figure 3, chapter 3.1) could have adsorbed more chloroform residues.

The PLA NFC/CTAB film shows amorphous properties with cold crystallization and enthalpy of fusion similar to those of the PLANFC/ZS1 film, and the mass loss (TG) is the lowest in the group of composites with the addition of surfactants ($\Delta m = -3.7\%$). The PLA NFC/P1670 film loses $\Delta m = 4.2\%$ of its weight during heating.

The above analysis of the thermal behaviour of all PLA films at 20-200 °C indicates that the addition of surfactant-modified cellulose nanofibers favours the retention of residual chloroform in the solvent-cast polymer film matrix and hinders its removal under vacuum conditions at ambient temperature.

3.4. Tensile properties of PLA NCF composite films

Tensile properties, such as: the tensile strength and elongation at break, of pure PLA in a crystalline and amorphous form and of PLA NFC composite films were evaluated. The results are summarized in Figure 8.

The tensile strength of neat PLA specimens in crystalline and amorphous forms were $42,0 \pm 2,4$ MPa, and $37,0 \pm 2,4$ MPa, respectively. Xu Zhang and Xiao Chen obtained slightly lower values of this parameter for foils of the PLA 6000 series but formed from a molten state at various crystallization temperatures (max. 29,4 MPa; min. 12,4 MPa). The authors pointed out that the strength of the cast foils decreased with the increase of the process temperature, and the highest result was obtained for the amorphous form (after rapid cooling). The result was explained by the spherulitic nature of the PLA crystals in the polymer matrix. Many nuclei are formed at a lower temperature, but spherulites increase in size as the crystallization temperature increases. At high temperature, spherulites become larger and irregular, and crystalline and amorphous regions begin to form two separate phases, deteriorating the mechanical properties of polymeric films [36]. In our study, the crystal structure of neat PLA was more robust than the amorphous form in solvent-cast film samples, indicating stronger interactions between ordered crystalline domains.

All composite PLA NFC samples had a lower tensile strength than both pure PLA control samples, especially with respect to the reference sample of crystalline PLA prepared under the same conditions (vacuum post-processing). The tensile strengths measured are $32,8 \pm 4,9$ MPa for PLA NFC/0 films with non-modified cellulose nanofibers and $31,5 \pm 2,8$ MPa, $31,0 \pm 2,3$ MPa and $34,1 \pm 1,5$ MPa for samples with surfactant-modified cellulose, i.e. PLA NFC/ZS1, PLA NFC/CTAB and PLANFC/P1670, respectively. These differences were small or non-existent taking into account measurement error. Hence, it is very likely that the cellulose nanofibers in the PLA matrix limited the free diffusion of chloroform between the polymer chains, which slowed down the process of film ordering and strengthening.

Chloroform residues interacting strongly with the polymer matrix (high desolvation temperatures by TGA analysis) can also play a role in both strengthening and plasticizing the film, as evidenced by measurements of the sample's elongation at break.

The elongation at break for crystalline PLA reached as much as 63.2 %, at which the solvent release temperature was the highest among all films. For amorphous PLA film, this parameter was about 7.92 %; but this is still higher than for samples containing cellulose nanofibrils. It should be noted that this sample was prepared without vacuum treatment and contained residual chloroform with

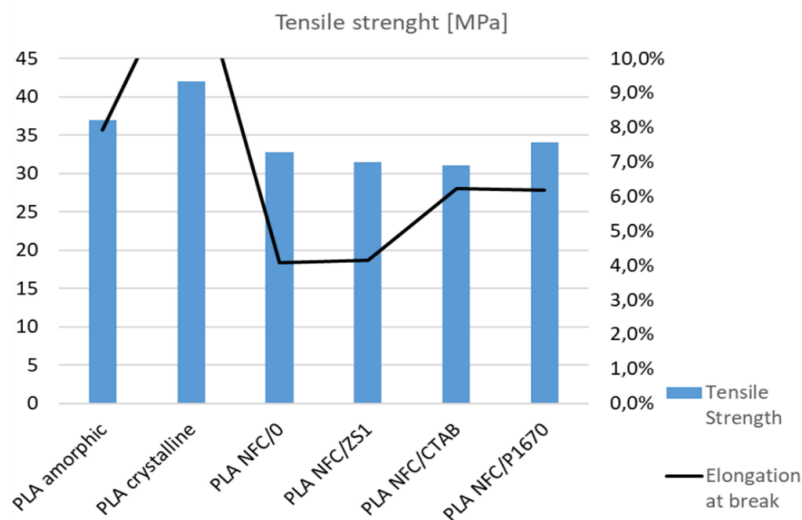


Fig. 8. Tensile strength and elongation at break of neat PLA and PLA/NFC composite films

varying degrees of interaction with the PLA chains.

Analyzing the effect of cellulose nanofibers and surfactants on the mechanical properties of composite films, the effect of the content and interaction of solvent residue molecules in the PLA matrix is also clearly visible. The elongation at break for the PLA NFC/0 sample was 4.07 %, similar to that of PLA NFC/ZS1 film, with a value of 4.15 %.

To sum up, the addition of surfactants does not increase the support function of NFC in PLA foil, although CTAB and P1670 may have an indirect plasticizing effect on the composite obtained through stronger bonding of chloroform molecules. Such an effect was not observed in the case of NFC modification with the ZS1 surfactant.

3.5. Disintegrability in composting of PLA and PLA/NFC composites

Disintegrability is expressed as a percentage and calculated as the ratio of the mass of the sample after a specific incubation time in simulated aerobic composting conditions to the mass of the starting sample.

In our study, we used the procedure described by Luzi *et al.* [37]. The

disintegration tests were carried out in a controlled environment, at a temperature of $58 \pm 2^\circ\text{C}$ and humidity of 40 – 65 %.













Under the influence of moisture and heat, PLA decomposition begins with adsorption and then the diffusion of water into the material. At first, the structure of the polymeric materials loosens because water molecules penetrating the matrix weaken and/or interrupt non-covalent interactions between polymer chains. This step depends on the ability and speed of water adsorption on the polymer surface. In the next stage, the separated polymer chains are cleaved into smaller fragments and/or lactic acid monomers by hydrolysis of ester groups. Hydrolysis is an autocatalytic process because the unblocked carboxyl groups accelerate the decomposition of subsequent ester groups in PLA. This step may be related to the rate of water diffusion in the polymer matrix. Finally, microorganisms present in the soil decompose these polymer residues into carbon dioxide, water and humus.

The decomposition of pure PLA films and PLA composites with cellulose modified with different types of surfactants was analyzed by observing changes in the appearance and weight of the tested samples after 2 weeks and after 3 weeks of storage in soil. After this time, the samples were sieved, dried and weighed. The effects of the samples' decomposition and percentage weights loss are shown in Figure 9.

After 3 weeks of storage in compost soil, the highest weight loss, almost 90 %, was recorded for the pure PLA sample in amorphous form, which was a predictable result compared to the crystalline form. Greater crystallinity gives the polymer a more ordered structure, which significantly limits the diffusion of water into the matrix and reduces the susceptibility to hydrolysis of polymer chains.

Meanwhile, all PLA composite films, both containing native cellulose nanofibers and modified with surfactants, turned out to be more resistant to decomposition in composting conditions. The lowest degree of sample decomposition after 3 weeks of being in the soil was recorded for the composite film with the unmodified cellulose composite, PLA NFC/0, and with cellulose modified with a non-ionic surfactant, PLA NFC/P1670. The best results in the disintegration of PLA/NFC/surfactant composites were obtained for samples containing ionic modifiers, such as cationic CTAB and anionic ZS1 surfactants. Research reports on the impact of cellulose fibers on biodegradation are very different and sometimes contradictory, as excellently summarized in a comprehensive review by Hubbe *et al.* [38].

The addition of cellulose to PLA generally hinders the diffusion of water into the polymer matrix. According to Jon Trifol *et al.* the presence of cellulose nanoparticles induces a crystalline structure that more effectively increases the barrier properties of the composite [39]. In our tests, cellulose did not have a significant effect on the crystallinity of the composites prepared. All PLA films with NFC and NFC/surfactant additives were amorphous (see chapter 3.2). In our opinion, unblocked and available – OH groups of cellulose chains can also effectively retain water and slow down its spread into the composite. The treatment of cellulose with a surfactant changes the nature of the surface of cellulose fibers, which promotes the rate of disintegration of the PLA/cellulose composite [37]. Additionally, the disintegrability increases with the value of the HLB surfactant parameter, which was also confirmed by our results [40].

PLA <i>crystalline</i>	PLA <i>amorphous</i>	PLA NFC/0	PLA NFC/ZS1	PLA NFC/CTAB	PLA NFC/P1670
After 2 weeks / weight loss					
					
-4,9%	-13,1%	-6,62%	-7,60%	-10,9%	-6,92%
After 3 weeks / weight loss					
					
-35,4%	-87,6%	-11,6%	-22,0%	-27,4%	-10,5%

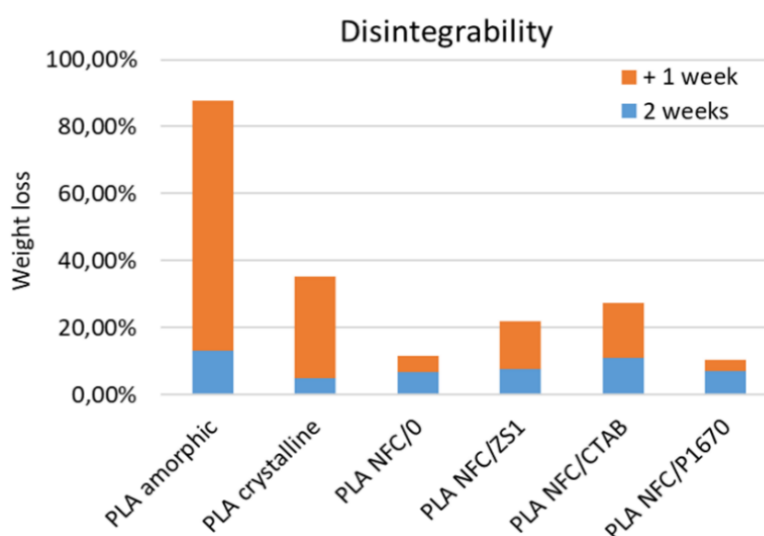


Fig. 9. Photos and diagram of mass loss of composite foils and reference samples of pure PLA crystalline and PLA amorphous forms after 2 and 3 weeks of composting

It is worth noting that the differences in the disintegration of all samples after the first 2 weeks in the soil were small, although the trend was consistent with predictions. A noticeable change in the rate of weight loss of the samples tested occurred in the following week, especially in the case of crystalline PLA films, as a result of autocatalyzed hydrolysis of ester bonds in PLA chains undisturbed by additives that can block access to free -OH and -COOH groups (see Figure 10). The terminal OH group of the lactic acid oligomer was found to play an important role in the decomposition of the polymer matrix, both in alkaline and acidic media. As mentioned by de Jong et al. protection of these hydroxyl groups results in significantly delayed degradation [41].

It is known that PLA degradation occurs mainly in the amorphous part of the polymer material. The high optical purity of the polymer significantly hinders crystallization, therefore the lower the content of the d-lactide isomer, the greater the tendency to form and retain an amorphous phase.

Gieldowska et al. conducted research on the hydrolytic degradation of fibers made of various types of PLA available on the market (Ingeo series, 4060D, 2002D and 6201D, i.e. with different contents of the D-lactide isomer). The authors showed that the amount of d-lactide isomer in the fibrous material has a significant impact on degradation, with a low d-lactide content leading to faster irreversible changes [42]. In our study we used PLA

Ingeo™ 6201D, which is characterized by a low share of the D-lactide isomer in the mass, approximately 1.4 %. For comparison, PLA Ingeo™ 4060D and PLA Ingeo™ 2002D contain 12 % and 2.5 % of the D-lactide isomer, respectively. It seems that the disintegration tendency of PLA 6000 series materials is mainly determined by this parameter, with almost 90 % degradation of the amorphous form of pure PLA. Nevertheless, the introduction of modified cellulose fibers into the polymer matrix, especially with ionic surfactants, supports the degradation of PLA NFC composites as compared to those containing cellulose fibers in their native form.

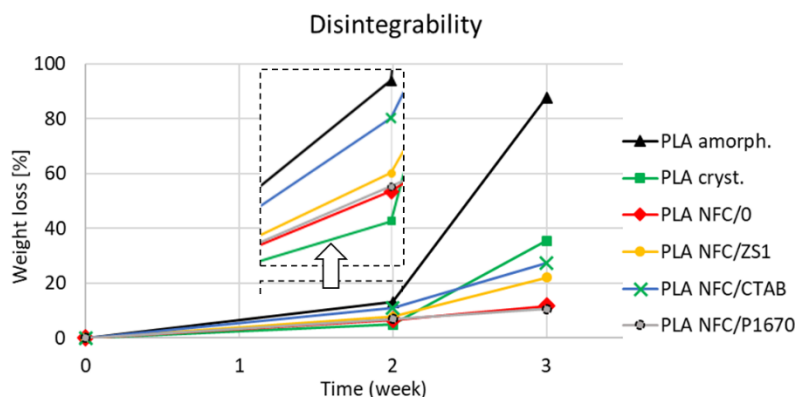


Fig. 10. Disintegrability of PLA NFC composites and reference samples of pure PLA films over time

4. Conclusions

Various types of polymer material available on the market (e.g. PLA Ingeo™ biopolymer) are intended for processing by various methods. According to the manufacturer, the Ingeo™ biopolymer PLA 2000 series is dedicated to extrusion/thermoforming, the Ingeo™ biopolymer PLA 3000 series - injection molding, the Ingeo™ biopolymer PLA 4000 series - film and sheet forming, and the Ingeo™ biopolymer PLA 6000 series - fiber and non-woven fabric production. However, other non-specific applications may be found for each of the above polymers. The study conducted for PLA Ingeo™ 6201D shows that the use of methods developed by other researchers to fine-tune the properties of PLA specimens often gives results that are different than expected. Most of the studies involve films molded from PLA 2000 and or 4000 series, which, compared to the 6000 series, were characterized by, among other things, a higher D isomer content by weight of the polymer.

Poly(lactic acid) (PLA)/cellulose nanofiber (CNF) composite films were prepared by solution casting. The authors examined the influence of CNF on thermal and mechanical properties as well as disintegrability under composting conditions of PLA materials. Mechanical tests correlated with DSC and TGA analysis showed that the introduction of surfactant-modified NFC significantly increased the affinity of chloroform particles to the polymer matrix. The release of residual solvents from composite films, especially in the case of PLA NFC/CTAB and PLA NFC/P1670, occurs at higher temperatures and also results in greater elongation at break in tensile tests.

Powder X-ray diffraction analyzes showed that the addition of CNF did not affect PLA crystallization kinetics. Amorphous PLA had a natural tendency to crystallize under vacuum conditions. However, the changes in the PXRD spectra of PLA NFC/0, PLA/NFC PLA NFC/ZS1 and PLA NFC/P1670 compared to the amorphous PLA sample were insignificant.

Modifying the surface of cellulose was intended to increase its dispersion in polymer matrices and thus maximize its reinforcing potential for polymer materials. There are many works confirming this thesis for film samples made of the PLA 2000 and 4000 series. Our research shows that the NFC particles were well dispersed in the PLA matrix, but for the polymer tested (PLA 6000 series) they did not have a reinforcing effect on the mechanical properties of the PLA NFC composite films produced.

Moreover, the degradation rate of polymer composites with cellulose under composting conditions is slower than in the case of pure PLA films, but the introduction of cellulose fibers modified with ionic surfactants in the polymer matrix has a supporting effect on the disintegrability.

Acknowledgements

This work partially was carried out within the project “Development of tailor-made PHB composites for technical applications“ PHB2MARKET – realized within the ERA-IB2 Programme, 7th Call, with financial support from Polish National Centre for Research and Development and German Federal Ministry of Education and Research.

The authors would like to thank Hanna Nosal and Marek Warzała (Łukasiewicz-Institute of Heavy Organic Synthesis, Kędzierzyn-Koźle, Poland) for kindly supplying partially saponified fatty acid methyl esters of castor oil (ZS1) and Jagoda Józwick-Pruska, Magdalena Szalczyńska and Piotr Cichacz for technical support.

References

- Gałęski A. (ed.): Stan i perspektywy rozwoju materiałów polimerowych (in Polish), CBMM PAN, Łódź (2008), chapter 4
- Trznadel M. Biorozkładalne materiały polimerowe (in Polish). *Polimery* 1995; 40(9): 485.
- Rasal RM, Janorkar AV, Hirt DE. Poly(lactic acid) modifications. *Prog Polym Sci* 2010; 35: 338–356.
- Gruber P. R. et al.; US 5142023, 1992
- Vatansever E, Arslan D, Nofar M. Poly(lactide) cellulose-based nanocomposites. *International Journal of Biological Macromolecules* 2019; 137: 912–938.
- Xiang Qi, Yiwei Ren, Xingzu Wang, New advances in the biodegradation of Poly(lactic) acid. *International Biodeterioration & Biodegradation* 2017; 117: 215–223.
- Pluta M. Morphology and properties of polylactide modified by thermal treatment, filling with layered silicates and plasticization, *Polymer* 2004; 45: 8239.
- Alvarado N, Romero J, Torres A, López de Dicastillo C, Rojas A, Galotto J, Guarda M. Supercritical impregnation of thymol in poly(lactic acid) filled with electrospun poly(vinyl alcohol)-cellulose

- nanocrystals nanofibres: Development an active food packaging material. *J Food Eng* 2018; 217: 1-10.
9. Rancan F, Papakostas D, Hadam S, Hackbarth S, Delair T, Primard C, et al. Investigation of polylactic acid (PLA) nanoparticles as drug delivery systems for local dermatotherapy. *Pharm Res* 2009; 26: 2027-2036.
 10. Savioli Lopes M., Jardini AL, Maciel Filho R. Poly(lactic acid) production for tissue engineering applications *Procedia Engineering* 2012; 42: 1402-1413.
 11. Pinar A, Mielička E. Assessment of Polylactide Properties for Use in Knitted Clothing Products. *Fibres Text East Eur* 2021; 29, 5(149): 66-74.
 12. Saeidlou S, Huneault MA, Li H, Park CB. Poly(lactic acid) crystallization. *Prog Polym Sci* 2012;37: 1657–1677
 13. Nofar M, Sacligil D, Carreau PJ, Kamal MR, Heuzey M-C. Poly (lactic acid) blends: processing, properties and applications. *Int J Biol Macromol* 2019; 125: 307–360.
 14. Nofar M, Park CB. Poly (lactic acid) foaming. *Prog Polym Sci* 2014;39: 1721–1741.
 15. Nofar M, Salehiyan R, Ray SS: Rheology of poly (lactic acid)-based systems. *Polym. Rev* 2019; 59 (3): 465-509.
 16. Li C., Sun C., Wang C., Tan H., Xie Y., Zhang Y. Cellulose nanocrystal reinforced poly(lactic acid) nanocomposites prepared by a solution precipitation approach. *Cellulose* 2020; 27: 7489–7502.
 17. Ilyas RA, Sapuan SM, Sanyang ML, Ishak, MR, Zainudin E. S.: Nanocrystalline cellulose as reinforcement for polymeric matrix nanocomposites and its potential applications: a review. *Curr Anal Chem* 2018; 14: 203–225.
 18. Nazrin A, Sapuan SM, Zuhri MYM, Ilyas RA, Syafiq R, Sherwani SFK. Nanocellulose Reinforced Thermoplastic Starch (TPS), Polylactic Acid (PLA), and Polybutylene Succinate (PBS) for Food Packaging Applications. *Frontiers in Chemistry* 2020; 8: Article 213.
 19. Kargarzadeh H, Huang J, Lin N, Ahmad I, Mariano M, Dufresne A, Galeski A. Recent developments in nanocellulose-based biodegradable polymers, thermoplastic polymers, and porous nanocomposites *Prog Polym Sci* 2018; 87: 197–227.
 20. Kyutoku H, Maeda N, Sakamoto H., Nishimura H, Yamada K. Effect of surface treatment of cellulose fibre (CF) on durability of PLA/CF bio-composites. *Carbohydr Polym* 2019; 203: 95–102
 21. Almási H, Ghanbarzadeh B., Dehghannya J., Entezami AA, Asl AK, Novel nanocomposites based on fatty acid modified cellulose nanofibres/poly(lactic acid): morphological and physical properties, *Food Packaging and Shelf Life* 2015; 5: 21–31.
 22. Ghasemi S, Behrooz R, Ghasemi I, Yassar RS, Long F. Development of nanocellulose-reinforced PLA nanocomposite by using maleated PLA (PLA-g-MA). *J Thermoplast Compos* 2018; 31, 1090–1101.
 23. Ling Z, Kai K, Ming-Bo Y, Wei Y. Recent progress on chemical modification of cellulose for high mechanical-performance Poly(lactic acid)/Cellulose composite. *Composites Communications* 2021;23: 100548.
 24. Lee JH, Park SH, Kim SH. Surface modification of cellulose nanowhiskers and their reinforcing effect in polylactide. *Macromol. Res.* 2014; 22: 424–430.
 25. Oksman K, Aitomäki Y, Mathew A, Siqueira G, Zhou Q, Butylina S, Tanpichai S, Zhou X, Hooshmand S. Review of the recent developments in cellulose nanocomposite processing, *Composites: Part A* 2016; 83: 2–18.
 26. Liu DY, Yuan XW, Bhattacharyya D, Easteal AJ. Characterisation of solution cast cellulose nanofibre - reinforced poly(lactic acid). *EXPRESS Polym Lett* 2010; 4 (1): 26–31.
 27. Orellana JL, Wichhart D, Kitchens ChL. Mechanical and Optical Properties of Polylactic Acid Films Containing Surfactant-Modified Cellulose Nanocrystals. *J Nanomater* 2018, Article ID 7124260, 12 pages.
 28. Wang Q, Ji Ch, Sun J, Zhu Q, Liu J. Structure and Properties of Polylactic Acid Biocomposite Films Reinforced with Cellulose Nanofibrils, *Molecules* 2020; 25: 3306.
 29. <https://www.natureworksllc.com/technology-and-products/products>
 30. Lee JH, Park SH, Kim SH. Preparation of cellulose nanowhiskers and their reinforcing effect in polylactide. *Macromol Res* 2013; 21: 1218–1225.
 31. Arslan D, Vatansever E, Sarul DS, Kahraman Y, Gunes G, Durmus A, Nofar M. Effect of preparation method on the properties of polylactide/cellulose nanocrystal nanocomposites, *Polymer Composites.* 2020;1–11.
 32. http://ifbb-knvb.wp.hs-hannover.de/db/files/downloads/TechnicalDataSheet_6201D_fiber-melt-spinning_pdf_1430990927.pdf
 33. Józwicka J, Gzyra-Jagięła K, Gutowska A, Twarowska-Schmidt K, Ciepłiński M. Chemical Purity of PLA Fibres for Medical Devices. *Fibres Text East Eur.* 2012; 20: 135 —141.
 34. Park S, Baker JO, Himmel ME, Parilla PA, Johnson DK. Cellulose crystallinity index: measurement techniques and their impact on interpreting cellulase performance. *Biotechnol Biofuels* 2010; 3: 10.
 35. Checchetto R, Rigotti D, Pegoretti A, Miotello A. Chloroform desorption from poly(lactic acid) nanocomposites: a thermal desorption spectroscopy study. *Pure Appl Chem* 2020; 92(3): 391–398.
 36. Ma B, Wang X, He Y, Dong Z, Zhang X, Chen X, Liu T. Effect of poly(lactic acid) crystallization on its mechanical and heat resistance performances *Polymer* 2021; 212: 123280.
 37. Luzi F, Fortunati E, Puglia D, Petrucci R, Kenny JM, Torre L. Study of disintegrability in compost and enzymatic degradation of PLA and PLA nanocomposites reinforced with cellulose nanocrystals extracted from *Posidonia Oceanica*. *Polym Degrad Stabil* 2015; 121: 105–115.
 38. Hubbe MA, Lavoine N, Lucia LA, Dou C. Formulating bioplastic composites for biodegradability, recycling, and performance: A Review *BioResources* 16; 1 2021-2083.
 39. Trifol J, Plackett D, Szabo P, Daugaard AE, Baschetti MG. Effect of Crystallinity on Water Vapor Sorption, Diffusion, and Permeation of PLA-Based Nanocomposites. *ACS Omega* 2020; 5 (25): 15362-15369
 40. Gois G, Santos A, Hernández E, Medeiros E, Almeida Y. Biodegradation of PLA/CNC composite modified with non-ionic surfactants. *Polym. Bull.* 2023; 80: 11363–11377.
 41. de Jong SJ, Arias ER, Rijkers DTS, van Nostrum CF, Kettenes-van den Bosch

- JJ, Hennink WE. New insights into the hydrolytic degradation of poly(lactic acid): participation of the alcohol terminus, *Polymer*, 2001; 42 (7): 2795-2802.
42. Gieldowska M, Puchalski M, Sztajnowski S, Krucińska I. Evolution of the Molecular and Supramolecular Structures of PLA during the Thermally Supported Hydrolytic Degradation of Wet Spinning Fibers *Macromolecules* 2022; 55 (22): 10100–10112.